

# Tuning Delocalization in the Radical Cations of 1,4-Bis[4-(diarylamino)styryl]benzenes, 2,5-Bis[4-(diarylamino)styryl]thiophenes, and 2,5-Bis[4-(diarylamino)styryl]pyrroles through Substituent Effects

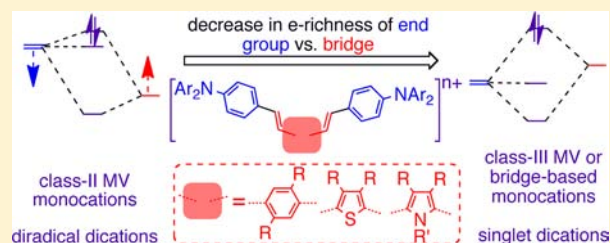
Stephen Barlow,\* Chad Risko, Susan A. Odom, Shijun Zheng, Veaceslav Coropceanu, Luca Beverina, Jean-Luc Brédas, and Seth R. Marder

Center for Organic Photonics and Electronics and School of Chemistry and Biochemistry, Georgia Institute of Technology, Atlanta, Georgia 30332-0400, United States

**S** Supporting Information

**ABSTRACT:** Radical cations have been generated for 10 bis[4-(diarylamino)styryl]arenes and heteroarenes to investigate the effect of the electron-richness of the terminal groups and of the bridging (hetero)arene on delocalization. The intervalence charge-transfer bands of these radical cations vary from weak broad Gaussians, indicative of localized class-II mixed-valence species, to strong relatively narrow asymmetric bands, characteristic of delocalized class-III bis(diarylamino) species, to narrow symmetric bands in cases where the bridge contribution to the singly occupied molecular orbital is largest.

Hush analysis of these bands yields estimates of the electronic coupling varying from  $480\text{ cm}^{-1}$  (electron-poor bridge, most electron-rich terminal aryl groups) to  $1000\text{ cm}^{-1}$  (electron-rich bridge, least electron-rich termini) if the diabatic electron-transfer distance,  $R_{ab}$ , is equated to the N–N separation. Computational and electron spin resonance (ESR) evidence for displacement of the diabatic states into the bridge (reduced  $R_{ab}$ ) suggests that these values are underestimates and that even more variation is to be expected through the series. Several dication species have also been studied. The vis–NIR absorption of the dication of (*E,E*)-1,4-bis[4-[bis(4-*n*-butoxyphenyl)amino]styryl]-2,5-dicyanobenzene is seen at an energy similar to that of the strongest band in the spectrum of the corresponding weakly coupled monocation, with approximately twice the absorptivity, and its ESR spectrum suggests essentially noninteracting radical centers. In contrast, the electronic spectra of class-III monocations show no clear relationship to those of the corresponding dications, which ESR reveals to be singlet species.



## INTRODUCTION

Organic mixed-valence (MV) species consist of two or more linked organic redox centers with different formal oxidation states.<sup>1,2</sup> The electronic structure of a two-site MV species can be described in terms of the interaction of two different diabatic states in which the oxidation or reduction is localized on either of the two redox centers. The electronic coupling,  $V$ , between these two states, which can be evaluated from characteristics of the intervalence charge-transfer (IVCT) absorption characteristics following Hush,<sup>3</sup> is often stronger in organic MV species than for their inorganic counterparts.<sup>4</sup> Moreover, some organic MV species are relevant to materials chemistry: for example, the charge carriers in bis(triarylamine)-based hole-transport materials, such as the widely used 4,4'-bis(phenyl-*m*-tolylamino)biphenyl, TPD,<sup>5–8</sup> are the corresponding MV radical cations,<sup>9,10</sup> and the absorption characteristics of MV bis(triarylamine) radical cations generated by photoinduced electron transfer may be useful in optical limiting.<sup>11,12</sup> In addition to their relevance to materials chemistry, triarylamine redox centers are also attractive candidates for the study of MV phenomena since a wide variety of systems can be synthesized in a reasonably straightforward manner, especially using Pd-

catalyzed chemistry developed by Buchwald and Hartwig,<sup>13,14</sup> and since, if appropriately substituted, they form moderately stable radical cations under mild oxidation conditions.<sup>15,16</sup>

In many organic and inorganic MV systems, the redox centers—for example, metal atoms or triarylamines—are often sufficiently remote from one another to preclude direct overlap between orbitals localized on these centers. Electronic coupling can be considered as the result of interaction of bridge-based orbitals with the “redox group” orbitals.<sup>17</sup> In  $\pi$ -conjugated organic systems it is the highest filled and lowest empty bridge orbitals that are generally most important for oxidized and reduced species, respectively. The strength of the resultant electronic coupling is, therefore, expected to increase with increased interaction between local redox-center and bridge orbitals, this interaction increasing as the bridge-based orbitals approach the redox-center orbitals in energy, as shown schematically in Figure 1. A number of studies support this expectation, including several bis(triarylamine) MV systems. For example, the couplings found for the radical cations of

Received: March 14, 2012

Published: June 11, 2012

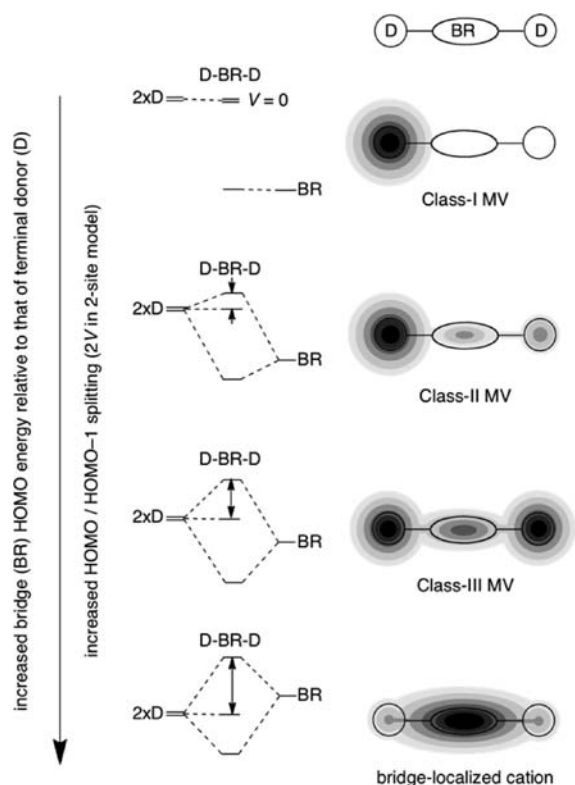
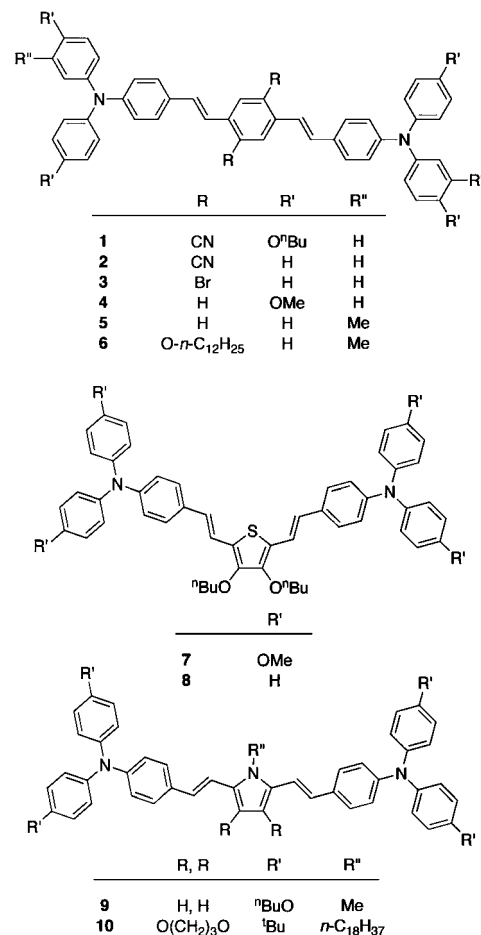


**Figure 1.** Schematic showing the anticipated effects of raising the energy of the highest occupied bridge-based orbital relative to those of terminal donors on (left) the highest filled orbitals of a neutral species and (right) the instantaneous spin distribution in the corresponding radical cation.

bis(diphenylamino)-terminated biphenyls or benzenes exceed those of their bis(di-*p*-anisylamino)-terminated analogues,<sup>10,18–20</sup> demonstrating the role of the electron-richness of the end group. The role of the bridge<sup>21</sup> is illustrated by work on the radical cations of bis[4-(di-*p*-anisylamino)phenyl]ethynyl]arenes with varying arene cores<sup>22,23</sup> and by the strong couplings observed in species incorporating thiophene groups in the bridge.<sup>24</sup> Inevitably, increasing coupling via bridging orbitals will lead to an increasing contribution of bridge orbitals to the singly occupied molecular orbital (SOMO); in other words, the oxidation (or reduction) acquires increased bridge character, or the redox center becomes displaced from its formal position into the bridge with a concomitant reduction in the diabatic electron-transfer distance,  $R_{ab}$ . Indeed, for bis(diarylamino) species, values of  $R_{ab}$  considerably reduced from the nitrogen–nitrogen separation are suggested by computational estimates<sup>25</sup> or are required for consistency between alternative experimentally based estimates of the electronic coupling,  $V$ .<sup>24–26</sup> Furthermore, density functional theory (DFT) calculations, supported by electron spin resonance (ESR) measurements, suggest that replacing the stilbene bridge of a bis(diarylamino) radical cation with a more electron-rich 1,2-dithienylethene bridge leads to an increase in the spin density on the bridge at the expense of that on the nitrogen atoms and the terminal aryl groups.<sup>24</sup> In the limiting case, the bridge contribution to the SOMO becomes sufficiently large that the radical ion is better described as the result of a bridge-based redox process (as shown schematically in Figure 1) than as being a true MV ion, as previously reported for several inorganic examples<sup>27,28</sup> and recognized as a possibility in bis(triarylamine) MV systems.<sup>23</sup>

Here we investigate the extent to which the electronic coupling in the radical cations of 1,4-bis[4-(diarylamino)styryl]benzenes and of related 2,5-bis[4-(diarylamino)styryl]-heteroarenes **1–10** (Chart 1) varies as the electron-richness of the terminal aryl groups and of the bridging 1,4-phenylene, 2,5-thienylene, or pyrrole-2,5-diyl groups is varied.

**Chart 1.** Structures of Bis[(diarylamino)styryl]benzenes, Bis[(diarylamino)styryl]thiophenes, and Bis[(diarylamino)styryl]pyrroles Discussed in This Work



## RESULTS AND DISCUSSION

**Compounds Investigated.** The syntheses of **1–9**<sup>25,26,29–34</sup> have previously been described. The terminal redox centers vary, in order of increasing electron-richness, from unsubstituted and alkyl-substituted 4-(diphenylamino)phenyl groups to the more electron-rich 4-[bis(4-alkoxyphenyl)amino]phenyl groups,<sup>35</sup> while the arenes/heteroarenes in the center of the bridge vary considerably in electron-richness from dicyanobenzene to an *N*-alkylpyrrole.<sup>36</sup> The new compound **10** incorporates the even more electron-rich *N*-alkyl-3,4-dialkoxypyrrole bridging group and was synthesized from the Horner reaction between the appropriate diethyl [(diarylamino)benzyl]phosphonate and pyrrole-2,5-dialdehyde (see the Supporting Information for details). Figure 2 shows the extent to which the electron-richness of end and bridging groups is varied among compounds **1–10**, as approximated by the highest occupied molecular orbital (HOMO) energies calculated at the B3LYP/6-31G(d) level for the triarylamine

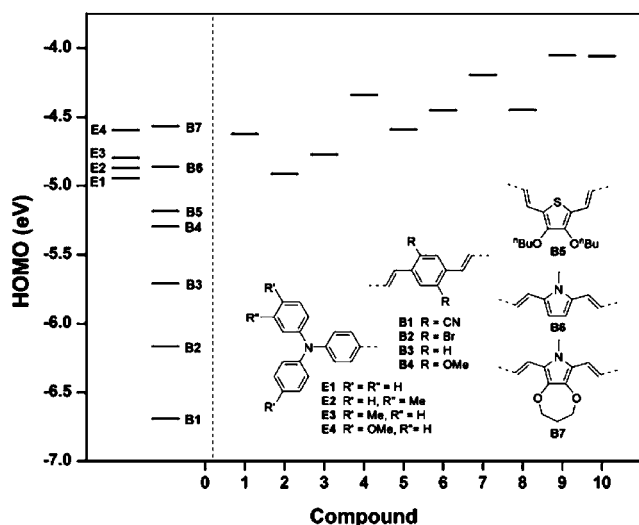


**Figure 2.** HOMO energies calculated at the B3LYP/6-31G(d) level of theory for compounds 1–10 and for the constituent end group (E1–E3) and bridging group (B1–B7) fragments (some alkyl groups have been replaced by methyl groups in the calculations).

(E1–E4) and divinylbenzene or divinylheterocycle (B1–B7) fragments. Solutions containing the corresponding radical cations and, in some cases (where solubility and stability allowed, specifically for 1, 4, 5, 6, 7, and 8), the dications were obtained in dichloromethane using tris(4-bromophenyl)aminium hexachloroantimonate ( $E_{1/2}^{+/0} = 0.70$  V vs  $\text{FeCp}_2^{+/0}$  in  $\text{CH}_2\text{Cl}_2$ <sup>37</sup>) as the oxidant. UV–vis–NIR and ESR data for 1<sup>+</sup>, 4<sup>+</sup>, 4<sup>2+</sup>, and 7<sup>2+</sup> have previously been published as parts of different studies.<sup>25,26,33</sup>

**Electrochemistry.** The redox potentials of the neutral species in dichloromethane are summarized in Table 1

**Table 1.** Electrochemical Half-Wave Potentials (V vs  $\text{FeCp}_2^{+/0}$ ,  $\text{CH}_2\text{Cl}_2/0.1$  M [ $^t\text{Bu}_4\text{N}^+$ ][ $\text{PF}_6^-$ ]) for 1,4-Bis[4-(diarylamino)styryl]benzenes and 2,5-Bis[4-(diarylamino)styryl]heteroarenes<sup>a</sup>

compound	+/0	2+/+	3+/2+
1	+0.26 <sup>b</sup>		+0.94
2	+0.51 <sup>b</sup>		–
3	+0.44 <sup>b</sup>		+1.06
4	+0.20 <sup>b</sup>		+0.81
5	+0.31 <sup>b</sup>		+0.97
6	+0.24 <sup>b</sup>		+0.91
7	+0.05 <sup>b</sup>		+0.70 <sup>c</sup>
8	+0.15 <sup>b</sup>		+0.97
9	–0.18	+0.01	+0.58
10	–0.26	–0.02	+0.73

<sup>a</sup>All processes were reversible. <sup>b</sup>Separation between first and second oxidations not resolved. <sup>c</sup>4+/3+ couple observed at +1.05 V.

(electrochemical data for 4 and 6–8 in dichloromethane have previously been reported,<sup>25,34</sup> while potentials in other solvents have also been reported for some of the other species<sup>29</sup>). Generally, the first and second electrons are removed at similar potentials, and the separation,  $\Delta E_{1/2} = E_{1/2}^{2+/+} - E_{1/2}^{+/0}$ , is not resolvable using cyclic voltammetry, the only exceptions being the pyrrole-based species 9 and 10, for which  $\Delta E_{1/2} = 0.19$  and 0.24 V, respectively; low to unresolvable values of  $\Delta E_{1/2}$  have been reported for other bis(triarylamine)s<sup>18</sup> and are not

surprising since electronic coupling generally makes only a small contribution to  $\Delta E_{1/2}$ ,<sup>38</sup> while electrostatic contributions, which can be important in systems where the charges are localized over a relatively small number of atoms and/or where the two redox centers are in close proximity, are likely to be small in the present systems.<sup>39</sup>

The  $E_{1/2}^{+/0}$  values reflect the overall electron-richness of the molecule and are consistent with expectations based on the electron-withdrawing or -donating character of the bridging and terminal substituents and on the relative ionization potentials of benzene, thiophene, and pyrrole.<sup>36</sup> The trends in  $E_{1/2}^{+/0}$  also agree well with those seen in the calculated HOMO energies (Figure 2). Moreover, comparison of the electrochemical potentials of 6–10 to those of model compounds in which the terminal diarylamino groups are replaced with *tert*-butyl groups indicates that the *difference* in potential between diamines and model compounds decreases as the core of the bridge is varied from dialkoxybenzene to dialkoxythiophene to pyrrole to dialkoxypyrrole (see Table S1 in the Supporting Information), suggesting increasing bridge character to the oxidation.

**Robin and Day Classification.** The lowest energy features of the electronic spectra of the radical cations (selected examples are shown in Figure 3; the remainder are shown in

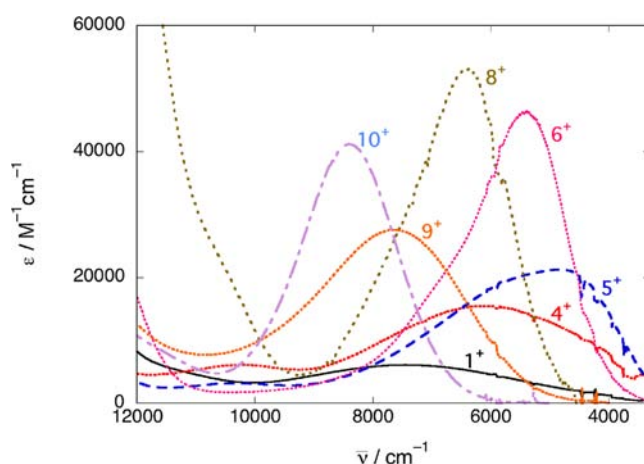


**Figure 3.** IVCT bands for selected bis[(diarylamino)styryl]benzene and bis[(diarylamino)styryl]heterocycle radical cations in  $\text{CH}_2\text{Cl}_2$ .

Figure S2 in the Supporting Information) are assigned to IVCT transitions. As shown in Table 2, those of 1<sup>+</sup>–4<sup>+</sup> are approximately symmetric Gaussians with widths at half-height,  $\bar{\nu}_{1/2}$ , exceeding the Hush limit of the following equation:

$$\bar{\nu}_{1/2}[\text{Hush}] = 4\sqrt{(\ln 2)\lambda k_B T} \quad (1)$$

where  $\lambda$  is the reorganization energy, which, for an MV compound in which charge is primarily localized on one of two equivalent redox centers, is equal to the IVCT absorption maximum,  $\bar{\nu}_{\text{max}}$ , thus suggesting that these species are Robin-and-Day<sup>40</sup> class-II MV compounds (as previously noted for 1<sup>+</sup> and 4<sup>+</sup> in refs 26 and 25, respectively). The IVCT band of 5<sup>+</sup> has neither the symmetric Gaussian line shape typical of class-II systems nor the characteristic shape of class-III bis-(triarylamine) MV IVCT bands (vide infra), presumably reflecting a species poised on the class-II/class-III borderline. The IVCT line shapes for 6<sup>+</sup>–8<sup>+</sup> are typical of those found for class-III bis(triarylamine)s,<sup>10,18,19,25</sup> i.e., narrower than the Hush limit expected for a class-II system (eq 1) and strongly

**Table 2. Experimental Parameters Characterizing the Intervalence Absorptions of the Radical Cations of Bis[(diarylamino)styryl]benzenes and Bis[(diarylamino)styryl]heterocycles in CH<sub>2</sub>Cl<sub>2</sub> with TD-DFT Gas-Phase Values in Italics<sup>a</sup> Along with Estimates of the Electronic Coupling**

	$\bar{\nu}_{\max}/\text{cm}^{-1}$	$\epsilon_{\max}/(10^3 \text{ M}^{-1} \text{ cm}^{-1})$	$\bar{\nu}_{1/2}[\text{obsd}]/\text{cm}^{-1}$	$\bar{\nu}_{1/2}[\text{Hush}]/\text{cm}^{-1}$	$\bar{\nu}_{1/2}[\text{high}]/\bar{\nu}_{1/2}[\text{low}]$	$\bar{\nu}_{1/2}[\text{high}]/\bar{\nu}_{1/2}[\text{Hush}]$	$\mu_{\text{ge}}/D$	$V_{\text{NN}}^b/\text{cm}^{-1}$	$V_{\text{class III}}^c/\text{cm}^{-1}$
1 <sup>+</sup>	7450 [4684]	6.1	4490 <sup>b</sup>	4150	1 <sup>d</sup>	1.08 <sup>d</sup>	5.78 <sup>d</sup> [21.0]	480	
2 <sup>+</sup>	5460 [5649]	14.2	4400	3550	0.96	1.21	7.91 [19.3]	480	
3 <sup>+</sup>	5300 [5962]	17.9	3980	3450	1.14	1.23	11.3 [19.0]	670	
4 <sup>+</sup>	6130 [5300]	15.5	4310 <sup>b</sup>	3760	1 <sup>d</sup>	1.15 <sup>d</sup>	10.3 <sup>d</sup> [21.1]	700	
5 <sup>+</sup>	4860 [6173]	21.3	3380	3350	2.15	1.38	11.8 [19.1]	640	
6 <sup>+</sup>	5400 6644	46.3	1980	3530	1.50	0.67	13.6 17.2	810	2700
7 <sup>+</sup>	5660 6280	45.8	2450	3620	1.81	0.97	13.9 16.6	960	2830
8 <sup>+</sup>	6390 7273	53.0	1980	3840	1.41	0.60	12.9 13.9	1000	3200
9 <sup>+</sup>	7630 6946	27.6	3090	4200	1.25	0.82	10.4 16.8	920	3820
10 <sup>+</sup>	8420 8018	41.1	1920	4410	1.01	0.44	9.65 14.3	940	4210

<sup>a</sup>TD-DFT values for 1<sup>+</sup>–5<sup>+</sup> are calculated for symmetrical DFT geometries, whereas the experimental data suggest that these cations belong to class-II; accordingly, the calculated  $\bar{\nu}_{\max}$  and  $\mu_{\text{ge}}$  values for those compounds cannot be directly compared to experiment and are given in brackets. <sup>b</sup>From eq 4 using experimental values of  $\bar{\nu}_{\max}$  and  $\mu_{\text{ge}}$  and equating  $R_{\text{ab}}$  to the N–N distance in the AM1 geometries of the neutral species. <sup>c</sup>From eq 3 using the experimental values of  $\bar{\nu}_{\max}$ . <sup>d</sup>Appears to be approximately symmetrical and assumed to be so due to overlap with other bands on the high-energy side.

asymmetric; the asymmetry has been explained in terms of coupling of the electron-transfer coordination to symmetric vibrational modes.<sup>19,41–43</sup> Compared to the IVCT bands of 6<sup>+</sup>–8<sup>+</sup>, that of 9<sup>+</sup> is less asymmetric and is broader, although still narrower than the Hush limit, and that of 10<sup>+</sup> is relatively narrow and essentially symmetrical.<sup>44</sup> The solvatochromic behavior of the IVCT bands of selected examples is also broadly consistent with the assignments to classes II and III (see the Supporting Information for details).

The structures of 1<sup>+</sup>–10<sup>+</sup> obtained from AM1/CI (CI = configuration interaction) calculations also suggest varying degrees of delocalization (see the Supporting Information for full details).<sup>45</sup> The structures of 1<sup>+</sup>–4<sup>+</sup> are markedly unsymmetrical. In the case of 1<sup>+</sup>, the oxidized amine is neither perfectly planar nor coplanar with the adjacent portion of the bridge; for this amine the N–C<sub>bridge</sub> bonds are longer and the terminal N–C<sub>aryl</sub> bonds shorter than those in the AM1 geometry of the corresponding neutral compound, and the distyrylbenzene bridge retains the twisted character seen in the neutral species, suggesting that the end groups for this cation play a more important role than the bridge in stabilizing the positive charge. The AM1/CI structures of 2<sup>+</sup> and 3<sup>+</sup> are qualitatively similar to that we have previously discussed for 4<sup>+</sup>:<sup>25</sup> one of the amines is coplanar with the adjacent stilbene unit of the bridge and exhibits N–C<sub>bridge</sub> and N–C<sub>aryl</sub> bonds shorter and longer, respectively, than those for the neutral species, while the rest of the structure resembles that of the neutral species. In contrast, the calculations suggest that oxidation of 5–10 results in both amino N–C<sub>bridge</sub> bonds shortening and all four terminal N–C<sub>aryl</sub> bonds lengthening, more planar distyryl(hetero)arene bridges, and planarization at both amine centers. However, except in the case of 9<sup>+</sup>, the C–N bond changes are more significant at one of the amine centers and the other amine center is somewhat twisted from coplanarity with the bridge, perhaps reflecting some residual tendency of the computational method toward overlocalization.<sup>46,47</sup> Nonetheless, the trends in the AM1/CI geometries are broadly consistent with the experimental results, with the compounds that experimentally appear to belong to class-II having the least planar and least symmetrical structures, while those that show class-III-like IVCT bands have structures that are more extensively planarized and more symmetrical.

**IVCT Bands and Electronic Coupling.** Compound 1 combines the most electron-rich terminal aryl groups and the most electron-poor bridging arylene group, and the IVCT band of 1<sup>+</sup> is the weakest of those studied, in terms of both absorptivity,  $\epsilon_{\max}$ , and transition dipole,  $\mu_{\text{ge}}$ . For compound 4<sup>+</sup>, the IVCT band is lower in energy and stronger than that of 1<sup>+</sup>, which has similar electron-rich end groups but a more electron-poor bridge. The increased strength can be attributed to increased electronic coupling,  $V$ , between the two diabatic states (vide infra). For a class-II system, the absorption maximum is equal to the reorganization energy associated with the intramolecular electron transfer,  $\lambda$ ; the external (solvent) contribution,  $\lambda_0$ , to  $\lambda$  is related to the *adiabatic* electron-transfer distance,  $R_{12}$ , according to

$$\lambda_0 = \frac{e^2}{4\pi} \left( \frac{1}{2a_1} + \frac{1}{2a_2} - \frac{1}{R_{12}} \right) \left( \frac{1}{n^2} - \frac{1}{D} \right) \quad (2)$$

where  $e$  is the electronic charge,  $a_1$  and  $a_2$  are effective radii of the two redox centers, and  $n$  and  $D$  are the solvent refractive index and dielectric constant, respectively.<sup>48</sup> Accordingly, the shift to lower IVCT transition energy between 1<sup>+</sup> and 4<sup>+</sup> may indicate a reduced value of  $R_{12}$ . Indeed, the AM1/CI calculations referred to above suggest that  $R_{12}$  decreases substantially (from 16.8 to 7.9 Å, Table S3 in the Supporting Information) between these two species.<sup>49</sup> Such a decrease in  $R_{12}$  can be attributed to (i) a reduced *diabatic* electron-transfer distance,  $R_{\text{ab}}$ , associated with increased delocalization of the diabatic states into the more electron-rich bridge and/or (ii) more ground-state delocalization between the two diabatic states associated with the increased  $V$ . A similar increase in  $\mu_{\text{ge}}$  and bathochromic shift of  $\bar{\nu}_{\max}$  and decrease in the AM1/CI estimate of  $R_{12}$  are seen on reducing the electron-richness of the terminal aryl groups, rather than increasing the electron-richness of the bridge, in 2<sup>+</sup> or 3<sup>+</sup> (Table 2; Table S3 and Figure 4, Supporting Information).

In class-III MV compounds, the IVCT absorption maximum is a direct measure of the electronic coupling<sup>50</sup> according to

$$2V = \bar{\nu}_{\max} \quad (3)$$

The experimental trends are consistent with the expected effects on  $V$  of varying the electron-richness of the terminal and

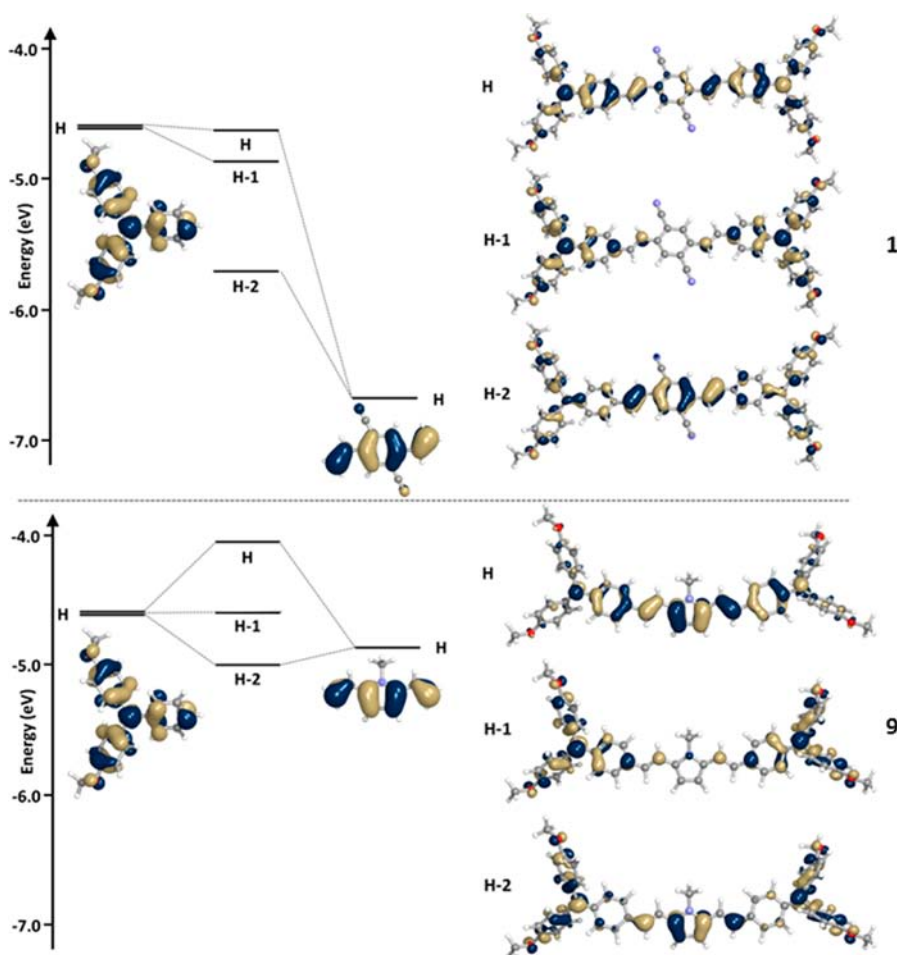


**Figure 4.** Representations of the three highest occupied orbitals of **1** and **9**, along with the HOMOs for fragments for the triarylamine and bridge groups, obtained at the B3LYP/6-31G(d) level of theory.

bridging groups. Thus, there are successive blue shifts in  $\bar{\nu}_{\max}$  from  $6^+$  to  $8^+$  to  $10^+$ , consistent with the expected increase in electron-richness from dialkoxybenzene to dialkoxythiophene to dialkoxy pyrrole; the blue shift seen between  $7^+$  and  $8^+$  can be attributed to the reduced electron-richness of the end groups, and the blue shift seen between  $9^+$  and  $10^+$  can be attributed to both the more electron-rich bridge and the less electron-rich end groups in the latter species. These shifts are all reproduced by time-dependent density functional theory (TD-DFT)/B3LYP calculations (Table 2), suggesting, as in some of our previous studies,<sup>24,51</sup> that although inappropriate for class-II systems,<sup>45</sup> this methodology can provide insight into the electronic properties of delocalized (class-III-like) species.<sup>52</sup> The TD-DFT-calculated transitions for these class-III species are, in each case, well-described as SOMO  $- 1 \rightarrow$  SOMO transitions, these orbitals corresponding closely to the (HOMO  $- 1$ )s and HOMOs, respectively, of the neutral species. For all compounds, the HOMO  $- 1$  and HOMO (Figure 4) can be regarded as combinations of the local HOMOs of the two triarylamine portions of the molecule: the HOMO  $- 1$  is essentially localized on the two triarylamine moieties, whereas the HOMO is an antibonding combination of the HOMO of the divinylarene/heterocycle of the bridge with the local HOMOs of the two triarylamines.<sup>53</sup> The relative bridge and triarylamine contributions to the HOMO vary considerably among the series: in the case of **1** the bridge contributions are minor and result primarily from the vinylene groups, whereas

for **9** and **10** the largest coefficients are on the pyrrole ring (Figure 4). Thus, although the calculations do confirm that the lowest energy transitions in each case have significant amine–amine IVCT character, they also suggest that, for the more strongly delocalized species, the band has significant amine  $\rightarrow$  bridge charge-transfer character. The important role played by the bridge in the IVCT bands of species such as  $9^+$  means that the two-site Hush model is of limited applicability: a complete treatment of these species would require consideration of the couplings between three sites—the two terminal redox sites and a bridge redox site—using an approach similar to that used in ref 23. However, parametrizing such a three-site model experimentally requires reliable assignment of, and reliable extraction of transition energies and transition dipole moments from, both electronic transitions between the resultant three potential surfaces. Accordingly, and to facilitate direct comparison with species such as  $1^+$ , which are much better approximated as two-site systems, in this study we limit our discussion to effective couplings extracted using a two-site treatment.

Finally,  $5^+$  shows the lowest energy IVCT maximum of any of the compounds investigated here. This is consistent with its assignment to either class-II or class-III; in the class-II case one would anticipate reduced  $R_{12}$  vs  $4^+$  due to the less electron-rich terminal aryl groups, whereas if  $5^+$  belongs to class-III, the apparent coupling would be expected to be smaller than that of  $6^+$ , in which the bridge is more electron-rich.

As noted above, the electronic coupling,  $V$ , between the two redox sites of a class-III system can be obtained directly from the IVCT absorption maximum. However, for both class-II and III species,  $V$  can be estimated from characteristics of the IVCT using the Hush expression

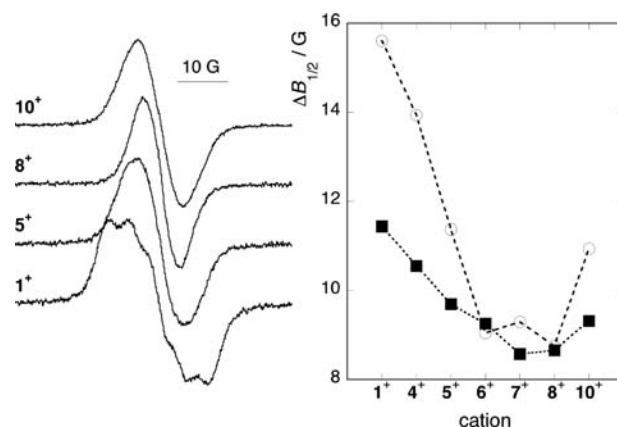
$$V = \frac{\mu_{ge} \bar{\nu}_{\max}}{eR_{ab}} \quad (4)$$

where  $e$  is the elementary charge and  $R_{ab}$  is the diabatic electron-transfer distance, i.e., the effective separation between the two redox sites in the absence of electronic coupling.<sup>54</sup> The values of  $V_{\text{NN}}$  given in Table 2 were obtained from eq 4 using  $\mu_{ge}$  and  $\bar{\nu}_{\max}$  taken from the experimental spectra and using the nitrogen–nitrogen distance,  $R_{\text{NN}}$ , for  $R_{ab}$ . The values generally increase down the series  $1^+–10^+$  as the bridge becomes more electron-rich, varying by a factor of ca. 2 between extremes, and are consistently larger for the experimentally class-III-like compounds  $6^+–10^+$  than for the class-II species  $1^+–4^+$ . This is broadly consistent with expectations based upon the electron-richness of terminal and bridging groups. The slight inconsistencies (for example, the experimentally indistinguishable estimates for  $1^+$  and  $2^+$ ) may reflect the (variable) discrepancy between  $R_{ab}$  and  $R_{\text{NN}}$  (vide infra); uncertainties in the determination of  $\mu_{ge}$  may also play a role, whereas in the case of  $5^+$  it is unclear how best to apply Hush theory to the unusual line shape of the IVCT band.

However, as noted in the Introduction, displacement of the diabatic states into the bridge means that  $R_{ab}$  is generally considerably less than  $R_{\text{NN}}$ , meaning that use of  $R_{\text{NN}}$  leads to underestimates of  $V$ . Indeed, we have previously reported computational estimates of  $R_{ab}$  for  $4^+$  that are 46–61% of  $R_{\text{NN}}$ ,<sup>25</sup> while we have used variable-temperature (VT) ESR to estimate a value for  $1^+$  that is 39% of  $R_{\text{NN}}$ .<sup>26</sup> For the species with class-III-like line shapes, coupling can also be estimated using eq 3; these values are given in Table 2 and indicate that use of  $R_{\text{NN}}$  both underestimates  $V$  and underestimates the variation of  $V$  between the class-III-like members of the series. The values of  $V_{\text{class III}}$  obtained from eq 3 are larger by a factor of ca. 3 ( $6^+–8^+$ ) or 4 ( $9^+$  and  $10^+$ ) than the values of  $V_{\text{NN}}$ , which may be compared to the factors of ca. 1.5–2 seen for class-III species with shorter bridges.<sup>24,25</sup> We have also computationally estimated  $R_{ab}$  for the present series (Table S3, Supporting Information), both from TD-DFT transition dipole moments, obtained at the symmetric DFT geometries,<sup>41,55</sup> and from the relationship among  $\mu_{ab}$ ,  $\mu_{ge}$ , and  $\Delta\mu_{12}$ ,<sup>56,57</sup> using experimental values of  $\mu_{ge}$  and AM1/CI values of  $\Delta\mu_{12}$ : the first approach gives values of  $R_{ab}$  that vary from ca.  $R_{\text{NN}}/2$  for  $1^+$  to ca.  $R_{\text{NN}}/3$  for  $10^+$ , while the second approach suggests variation from close to  $R_{\text{NN}}$  ( $1^+$ ) to ca.  $R_{\text{NN}}/4$  ( $10^+$ ). However, while the values estimated vary considerably with the specific approach,  $R_{ab}$  is found to generally decrease with more electron-rich bridging groups or more electron-poor end groups; i.e., the factors that lead to increased  $V$  also lead to reduced  $R_{ab}$ . Therefore, these computational estimates also suggest that use of  $R_{\text{NN}}$  leads not only to underestimates of  $V$ , but also to underestimates of the variation of  $V$  between the most weakly and most strongly coupled examples.

**Monocation Electron Spin Resonance Spectra and Spin Distribution.** As noted above, the SOMOs of the more delocalized examples are increasingly concentrated on the bridging groups, raising the question of the extent to which these radical cations can still be regarded as diamine MV

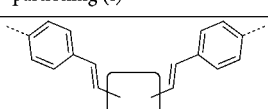
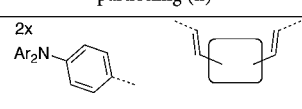
compounds. We have previously compared DFT-calculated and experimental values of ESR hyperfine coupling constants to establish that DFT gives a good description of the spin-density distribution in the radical cations of some bis(diarylamino) derivatives of thiophene-based bridges.<sup>24</sup> Such an approach is slightly less straightforward here in that the experimental ESR spectra (Figure 5; Figure S6, Supporting Information) display



**Figure 5.** Left: first-derivative ESR spectra of selected diamine radical cations in  $\text{CH}_2\text{Cl}_2$ . Right: line widths of ESR spectra of diamine radical cations obtained from experiment (open circles) and simulation based on DFT hyperfine coupling constants and a 0.5 G line broadening (solid squares).

little to no resolvable coupling and, in many cases, are structureless Gaussian absorptions: the previously reported room-temperature ESR spectra of  $1^+$  and  $4^+$  are characterized by poorly resolved coupling to two  $^{14}\text{N}$  centers (consistent with rapid intramolecular electron transfer between the two redox centers),<sup>26</sup> while spectra of  $5^+$ ,  $6^+$ ,  $7^+$ ,  $8^+$ , and  $10^+$  acquired under the same conditions show an even less well-resolved structure. However, there is considerable variation in the overall line width of the ESR signals from cation to cation. In principle, intermolecular exchange between cations and neutral species can lead to narrowing of spectra; however, such effects give rise to a Lorentzian line shape<sup>26,58</sup> and are not observed in related systems at comparable concentrations,<sup>24,26,58</sup> so it is assumed that the line widths are determined by the unresolved hyperfine coupling constants. Accordingly, hyperfine constants obtained from B3LYP/6-31G(d) calculations were used in combination with a constant Gaussian line broadening to simulate spectra using WinSIM;<sup>59–61</sup> the overall widths at half-height of the integrated spectra were then compared with those of the experimental integrated spectra. It should be noted that in all cases the calculated coupling constants were obtained for symmetrical DFT geometries, whereas NIR data (vide supra) and, for  $1^+$ , low-temperature ESR data<sup>26</sup> indicate some of the cations are class-II species, meaning that the calculations cannot describe the instantaneous spin distribution within these cations; however, we have previously shown that DFT can nonetheless give a reasonable description of the average coupling constants and, therefore, spin distribution resulting from intermolecular exchange.<sup>26</sup> As shown in Figure 5, both experimental and simulated line widths decrease in the order  $1^+ > 4^+ > 5^+ > 6^+$ ; experiment and simulations indicate similar line widths for  $6^+$ ,  $7^+$ , and  $8^+$  but disagree on the details, and finally, both experiment and simulation show an increased line width for  $10^+$  relative to  $7^+$  and  $8^+$ . The calculations indicate that

Table 3. Two Alternative Partitionings of the DFT-Calculated Spin Densities between Terminal and Bridging Groups of Diamine Radical Cations

	partitioning (i)		partitioning (ii)	
				
$1^+$	0.612	0.388	0.844	0.156
$2^+$	0.450	0.550	0.756	0.244
$3^+$	0.395	0.605	0.695	0.305
$4^+$	0.486	0.514	0.731	0.269
$5^+$	0.368	0.632	0.657	0.343
$6^+$	0.297	0.703	0.565	0.435
$7^+$	0.353	0.647	0.600	0.400
$8^+$	0.266	0.733	0.535	0.465
$9^+$	0.304	0.696	0.532	0.468
$10^+$	0.232	0.777	0.465	0.535

these trends in line width are primarily due to decreasing coupling to the diamine  $^{14}\text{N}$  nuclei ( $A_{\text{N}}$  is calculated to decrease from 3.44 G for  $1^+$  to 1.81 G for  $10^+$ ), opposed by increasing coupling to bridge nuclei (most dramatically the vinylenic  $^1\text{H}$  nuclei and, in the case of  $10^+$ , the pyrrole  $^{14}\text{N}$  nucleus, for which  $A_{\text{N}} = -1.44$  G); moreover, DFT is seen to provide a reasonable description of the spin distribution in these cations, consistent with the observation (vide supra) that TD-DFT transition energies for the delocalized examples are in reasonable agreement with experiment.

Table 3 summarizes how the DFT spin densities are distributed. The oxidation of  $1^+$  is the most strongly triarylamine-localized, with 84% of the spin density on these groups, but nonetheless shows some contribution from the divinylidicyanobenzene bridge, consistent with the reduced values of  $R_{\text{ab}}$  implied by some of the computational estimates (see above and the Supporting Information) and by previous VT-ESR studies.<sup>26</sup> The spin densities on the triarylamine moieties generally decrease down the series, with all experimentally class-III-like radical cations  $6^+–10^+$  showing reduced triarylamine spin density relative to their class-II counterparts ( $1^+–4^+$ ). Moreover, the successively increased bridge character of the oxidation seen among  $6^+$ ,  $8^+$ , and  $10^+$  (dialkoxybenzene vs dialkoxythiophene vs dialkoxyproline) is consistent with electrochemical comparisons to model compounds (vide supra; Table S1, Supporting Information). While there is no clear-cut criterion on what can and cannot be considered an MV compound, it is clear that MV character decreases down the series ( $1^+–10^+$ ) at the expense of bridge-centered oxidation. However, in all cases, apart from that of  $10^+$ , more than half the spin is located on the triarylamine units, indicating significant retention of MV character.

**Electronic and Electron Spin Resonance Spectra of the Dications.** For selected examples we have also obtained vis–NIR and ESR spectra of the corresponding dications. In addition to the low-energy bands assigned to IVCT discussed in the previous sections, the localized radical cations  $1^+–4^+$  (as well as the putatively borderline cation  $5^+$ ) all exhibit strong absorptions at 13000–15000  $\text{cm}^{-1}$  (see Figures S2 and S3 in the Supporting Information and the figures in refs 25 and 26) at energies similar to those of the absorptions of isolated triarylamine radical cations<sup>62–64</sup> and of bands observed for

other weakly coupled bis(triarylamine) radical cations, where they have previously been assigned to localized transitions within the  $\text{Ar}_2\text{N}^+$  units.<sup>18</sup> Figure 6 shows that, for **1**, the dication spectrum is dominated by an absorption at essentially the same energy as the “ $\text{Ar}_2\text{N}^+$ ” absorption of the monocation with

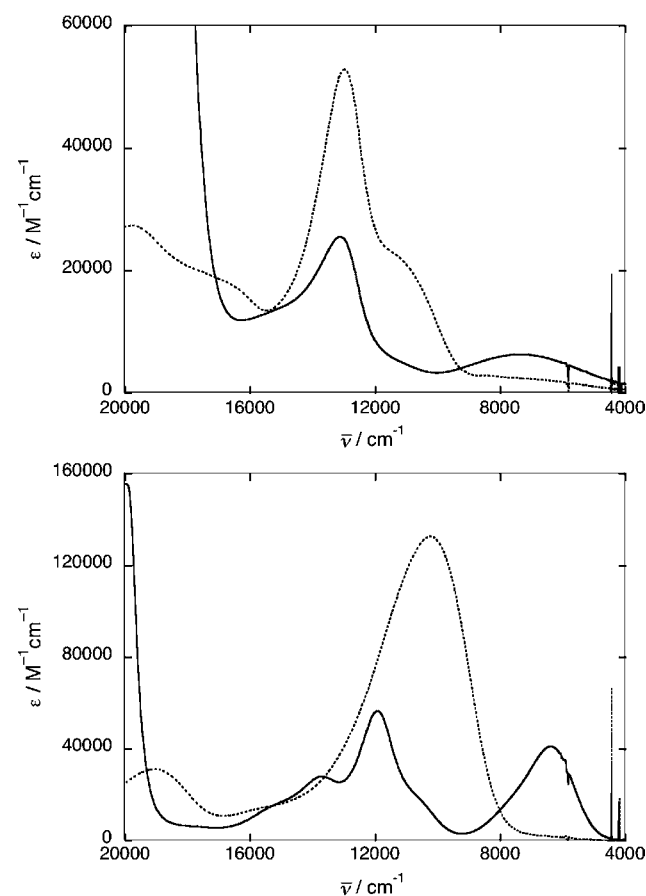


**Figure 6.** Vis–NIR absorption spectra of monocations (solid lines) and dications (broken lines) of **1** (above) and **8** (below) in  $\text{CH}_2\text{Cl}_2$ . The strong absorptions at high energy in the monocation spectra are due to the presence of an excess of the neutral species. Note the different vertical scales in the two graphs.

approximately twice the absorptivity,<sup>65</sup> suggesting the dication can be regarded as two more-or-less noninteracting triarylaminium units. This is consistent with the location of the  $1^{++}$  system toward the weakly coupled end of the class-II spectrum, where the redox centers are almost independent, so as described by Robin and Day,<sup>40</sup> apart from a weak IVCT band, the electronic spectrum of the MV species exhibits features characteristic of both the fully oxidized and reduced species (i.e., dication and neutral, respectively, in the present series). On the other hand, the spectrum of  $4^{2+}$  is not so clearly related to that of  $4^+$ , being dominated by a strong absorption at  $9300\text{ cm}^{-1}$  (Figure 2 of ref 25), similar to that seen for  $5^{2+}$ – $8^{2+}$  ( $9500$ – $10000\text{ cm}^{-1}$ ; Figure 6b; Figs S3–S5, Supporting Information), indicating deviation from the picture of non-interacting triarylaminium units. However, while  $4^{2+}$  also exhibits an “ $\text{Ar}_2\text{N}^+$ ” absorption in a position similar to that of the monocation,  $5^{2+}$ – $8^{2+}$  do not.<sup>66</sup>

Several limiting magnetic situations can be envisaged for dications of diamines: (a) strong ferromagnetic coupling resulting in an  $S = 1$  configuration, (b) strong antiferromagnetic coupling resulting in an  $S = 0$  situation, and (c) two independent  $S = 1/2$  radical centers (i.e., a vanishing energy gap between singlet and triplet). The first scenario is typically favored for systems in which the relevant orbitals are orthogonal, such as those with 1,3-phenylene bridges, whereas in the present systems with 1,4-phenylene (or pyrrole-2,5-diyl or 2,5-thienylene) bridges, singlet (b), “biradical” (c), or intermediate situations might be expected, depending on the degree of interaction between the redox centers. For several of the bis[(diarylmino)stryryl] compounds for which we were able to obtain reasonably stable dication solutions, we estimated room-temperature spin concentrations by double integration of the first-derivative ESR spectra. We have previously reported that  $7^{2+}$  is a singlet (ESR, NMR, comparison of bond lengths in the crystal structure with those calculated for various electronic configurations)<sup>33</sup> and that solutions of  $4^{2+}$  have a spin concentration according to ESR that corresponds to  $1.2 \pm 0.1 S = 1/2$  centers per molecule.<sup>25</sup> We found that  $5^{2+}$ ,  $6^{2+}$ , and  $8^{2+}$  are also essentially diamagnetic (consistent with the similarity of the electronic spectra of  $5^{2+}$ – $8^{2+}$ , vide supra).<sup>67</sup> On the other hand, the spin concentration measured by ESR for  $1^{2+}$  essentially corresponds to the “biradical” limit, consistent with the dication vis–NIR spectrum described above, which also suggests largely independent triarylaminium centers. Figure 7 compares the number of spins measured by room-temperature ESR for the dications with the electronic couplings estimated for the corresponding MV radical monocations using eq 4 and taking  $R_{\text{ab}} = R_{\text{NN}}$ . The figure clearly indicates that the trend in magnetic coupling in these dications parallels that in electronic coupling in the corresponding MV cations. We have previously made similar observations in a series of bis(di-*p*-anisylamino)-terminated oligo(phenylenevinylene)s with varying bridge length (compound 4 being a member of that series).<sup>25,68</sup> In both the previously studied and present series, for the species where  $V$  is sufficiently strong to lead to class-III MV behavior in the monocation, the magnetic coupling is sufficiently strong to result in a room-temperature singlet configuration for the dication.

## SUMMARY

We have varied the relative electron-richness of the terminal aryl and bridging arene/heteroarene groups in a series of

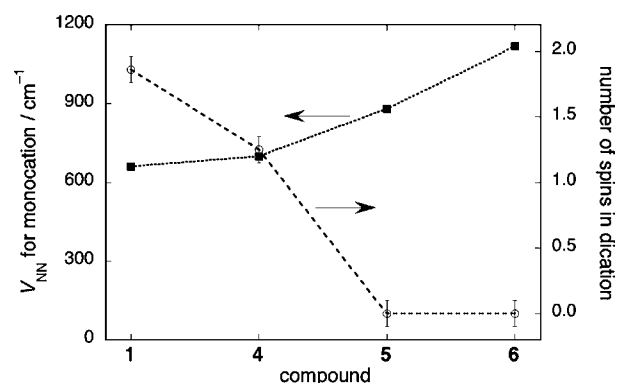


**Figure 7.** Comparison of electronic coupling in the monocation (solid squares), estimated using eq 4 and the N–N separation, with the number of spins per dication molecule (open circles), estimated by ESR, for some bis[(diarylmino)stryryl]benzenes. The dotted lines are provided as a guide to the eye but have no physical significance.

bis[(diarylmino)stryryl]arene/heteroarene radical cations. While a few previous studies have recognized the importance of relative bridge and end-group orbital energies in organic MV compounds, the present work includes more extensive variations of these relative energetics, resulting in a large variation in the delocalization behavior and a more comprehensive understanding of how this behavior can be controlled: a combination of experimental and computational data show that these cations can be tuned from weakly coupled strongly unsymmetrical class-II MV ions ( $1^+$ ), via more strongly coupled class-II species (e.g.,  $4^+$ ) and an apparently borderline case ( $5^+$ ), to delocalized symmetrical class-III MV-type species (e.g.,  $6^+$ ) and to symmetrical species that might arguably be better described as “bridge-based” ( $10^+$ ). Using a two-state Hush analysis of the lowest energy NIR transitions, the apparent electronic couplings between the redox centers,  $V$ , vary by at least a factor of ca. 2 when  $R_{\text{ab}}$  is assumed to be roughly constant. However, orbitals, spin densities (validated by comparison of DFT-simulated and experimental ESR spectra), and transition dipoles obtained from TD-DFT calculations indicate increasing displacement of the redox centers into the bridge as the bridge electron-richness is increased relative to that of the terminal groups, thus further accentuating the variation in  $V$ . The corresponding dications vary from diradicals, consisting of two weakly interacting triarylaminium moieties, to singlets (i.e., strong antiferromagnetic coupling), the trends in magnetic coupling in the dications paralleling those in electronic coupling in the radical cations.

## ASSOCIATED CONTENT

### Supporting Information

Experimental details for synthesis, mono- and dication characterization, and quantum chemical calculations, additional electrochemical data, figures showing additional complete mono- and dication spectra, solvatochromic data for selected cations, computational estimates of geometric and electron-transfer distances and of electronic coupling, computed geometric parameters, and XYZ coordinates and absolute energies (hartrees) for the DFT-optimized geometries of the neutral and radical cation species. This material is available free of charge via the Internet at <http://pubs.acs.org>.



## ■ AUTHOR INFORMATION

## Corresponding Author

stephen.barlow@chemistry.gatech.edu

## Notes

The authors declare no competing financial interest.

## ■ ACKNOWLEDGMENTS

This work was supported by the National Science Foundation, through the Science and Technology Center Program (Grant DMR-0120967) and a Graduate Research Fellowship to S.A.O., and by the Office of Naval Research, through the DARPA MORPH Program (Grant N-00014-06-1-0897). Part of the computational resources have been provided by Georgia Tech's Center for Computational Molecular Science and Technology, which is funded through a NSF CRIF award (Grant No. CHE-0946869) and by the Georgia Institute of Technology. We also thank S. Thaymanavan and Michael D. Levin for the syntheses of 1–3 and John R. Reynolds for a gift of an intermediate used to obtain 10.

## ■ REFERENCES

- Hankache, J.; Wenger, O. S. *Chem. Rev.* **2011**, *111*, 5138.
- Heckmann, A.; Lambert, C. *Angew. Chem., Int. Ed.* **2012**, *51*, 326.
- Hush, N. S. *Prog. Inorg. Chem.* **1967**, *8*, 391.
- Nelsen, S. F.; Tran, H. Q.; Nagy, M. A. *J. Am. Chem. Soc.* **1998**, *120*, 298.
- Tang, C. W.; Van Slyke, S. A. *Appl. Phys. Lett.* **1987**, *51*, 913.
- Kido, J.; Kimura, M.; Nagai, K. *Science* **1995**, *267*, 1332.
- Bulovic, V.; Gu, G.; Burrows, P. E.; Forrest, S. R.; Thompson, M. E. *Nature* **1996**, *380*, 29.
- Borsenberger, P. M.; Weiss, D. S. *Organic Photoreceptors for Xerography*; Marcel Dekker: New York, 1998.
- Littleford, R. E.; Paterson, M. A. J.; Low, P. J.; Tackley, D. R.; Jayes, L.; Dent, G.; Cherryman, J. C.; Brown, B.; Smith, W. E. *Phys. Chem. Chem. Phys.* **2004**, *6*, 3257.
- Low, P. J.; Paterson, M. A. J.; Puschmann, H.; Goeta, A. E.; Howard, J. A. K.; Lambert, C.; Cherryman, J. C.; Tackley, D. R.; Leeming, S.; Brown, B. *Chem.—Eur. J.* **2004**, *10*, 83.
- Spangler, C. W. *J. Mater. Chem.* **1999**, *9*, 2013.
- Huang, C.; Sartin, M. M.; Siegel, N.; Cozzuol, M.; Zhang, Y.; Hales, J. M.; Barlow, S.; Perry, J. W.; Marder, S. R. *J. Mater. Chem.* **2011**, *21*, 16119.
- Wolfe, J. P.; Wagaw, S.; Buchwald, S. L. *J. Am. Chem. Soc.* **1996**, *118*, 7215.
- Driver, M. S.; Hartwig, J. F. *J. Am. Chem. Soc.* **1996**, *118*, 7217.
- Seo, E. T.; Nelson, R. F.; Fritsch, J. M.; Marcoux, L. S.; Leedy, D. W.; Adams, R. N. *J. Am. Chem. Soc.* **1966**, *88*, 3498.
- Dapperheld, S.; Steckhan, E.; Grosse-Brinkhaus, K.-H.; Esch, T. *Chem. Ber.* **1991**, *124*, 2557.
- Brunschwig, B. S.; Creutz, C.; Sutin, N. *Chem. Soc. Rev.* **2002**, *31*, 168.
- Lambert, C.; Nöll, G. *J. Am. Chem. Soc.* **1999**, *121*, 8434.
- Szeghalmi, A. V.; Erdmann, M.; Engel, V.; Schmitt, M.; Amthor, S.; Kriegisch, V.; Nöll, G.; Stahl, R.; Lambert, C.; Leusser, D.; Stalke, D.; Zabel, M.; Popp, J. *J. Am. Chem. Soc.* **2004**, *126*, 7834.
- Coropceanu, V.; Gruhn, N. E.; Barlow, S.; Lambert, C.; Durivage, J. C.; Bill, T. G.; Nöll, G.; Marder, S. R.; Brédas, J.-L. *J. Am. Chem. Soc.* **2004**, *126*, 2727.
- Other features of bridging groups besides their local orbital energies can play a role in determining electronic coupling. For example, the radical cation of 9,10-bis[bis(4-methoxyphenyl)amino]anthracene radical cation is less strongly coupled than its *p*-phenylene-bridged analogue due to the disruption of orbital overlap through steric effects: Lambert, C.; Risko, C.; Coropceanu, V.; Schelter, J.; Amthor, S.; Gruhn, N. E.; Durivage, J. C.; Brédas, J. L. *J. Am. Chem. Soc.* **2005**, *127*, 8508.
- Lambert, C.; Nöll, G.; Schelter, J. *Nat. Mater.* **2002**, *1*, 69.
- Lambert, C.; Amthor, S.; Schelter, J. *J. Phys. Chem. A* **2004**, *108*, 6474.
- Odom, S. A.; Lancaster, K.; Beverina, L.; Lefler, K. M.; Thompson, N. J.; Coropceanu, V.; Brédas, J.-L.; Marder, S. R.; Barlow, S. *Chem.—Eur. J.* **2007**, *13*, 9637.
- Barlow, S.; Risko, C.; Chung, S.-J.; Tucker, N. M.; Coropceanu, V.; Jones, S. C.; Levi, Z.; Brédas, J. L.; Marder, S. R. *J. Am. Chem. Soc.* **2005**, *127*, 16900.
- Lancaster, K.; Odom, S. A.; Jones, S. C.; Thayumanavan, S.; Marder, S. R.; Brédas, J. L.; Coropceanu, V.; Barlow, S. *J. Am. Chem. Soc.* **2009**, *131*, 1717.
- Kaim, W. *Inorg. Chem.* **2011**, *50*, 9752 and references therein.
- Roussel, P.; Cary, D. R.; Barlow, S.; Green, J. C.; Varret, F.; O'Hare, D. *Organometallics* **2000**, *19*, 1071.
- Pond, S. J. K.; Rumi, M.; Levin, M. D.; Parker, T. C.; Beljonne, D.; Day, M. W.; Brédas, J. L.; Marder, S. R.; Perry, J. W. *J. Phys. Chem. A* **2002**, *106*, 11470.
- Frederiksen, P. K.; Jørgensen, M.; Ogilby, P. R. *J. Am. Chem. Soc.* **2001**, *123*, 1215.
- Kauffman, J. M.; Moyna, G. *J. Org. Chem.* **2003**, *68*, 839.
- Rumi, M.; Ehrlich, J. E.; Heikal, A. A.; Perry, J. W.; Barlow, S.; Hu, Z.; McCord-Maughon, D.; Parker, T. C.; Röckel, H.; Thayumanavan, S.; Marder, S. R.; Beljonne, D.; Brédas, J.-L. *J. Am. Chem. Soc.* **2000**, *122*, 9500.
- Zheng, S.; Barlow, S.; Risko, C.; Kinnibrugh, T. L.; Khurstalev, V. N.; Antipin, M. Y.; Tucker, N. M.; Timofeeva, T.; Coropceanu, V.; Jones, S. C.; Brédas, J.-L.; Marder, S. R. *J. Am. Chem. Soc.* **2006**, *128*, 1812.
- Zheng, S.; Beverina, L.; Barlow, S.; Zojer, E.; Fu, J.; Padilha, L. A.; Fink, C.; Kwon, O.; Yi, Y.; Shuai, Z.; Van Stryland, E. W.; Hagan, D. J.; Brédas, J.-L.; Marder, S. R. *Chem. Commun.* **2007**, 1372.
- Kwon, O.; Barlow, S.; Odom, S. A.; Beverina, L.; Thompson, N. J.; Zojer, E.; Brédas, J.-L.; Marder, S. R. *J. Phys. Chem. A* **2005**, *109*, 9346.
- The ionization energies of pyrrole and thiophene are 8.9 and 8.2 eV, respectively (Sell, J. A.; Kuppermann, A. *Chem. Phys. Lett.* **1978**, *61*, 355), although a smaller difference might be expected between pyrrole and dialkoxythiophene. We have previously noted that alkylpyrrole derivatives are more readily oxidized than their dialkoxythiophene analogues (see ref 34 and Zheng, S.; Leclercq, A.; Fu, J.; Beverina, L.; Padilha, L. A.; Zojer, E.; Schmidt, K.; Barlow, S.; Luo, J.; Jiang, S.-H.; Jen, A. K.-Y.; Yi, Y.; Shuai, Z.; Van Stryland, E. W.; Hagan, D. J.; Brédas, J.-L.; Marder, S. R. *Chem. Mater.* **2007**, *19*, 432).
- Connelly, N. G.; Geiger, W. E. *Chem. Rev.* **1996**, *96*, 877.
- Sutton, J. E.; Taube, H. *Inorg. Chem.* **1981**, *20*, 3125.
- Ribou, A. C.; Launay, J.-P.; Sachtleben, M. L.; Li, H.; Spangler, C. W. *Inorg. Chem.* **1996**, *35*, 3735.
- Robin, M. B.; Day, P. *Adv. Inorg. Chem. Radiochem.* **1967**, *10*, 247.
- Coropceanu, V.; Malagoli, M.; André, J. M.; Brédas, J. L. *J. Am. Chem. Soc.* **2002**, *124*, 10519.
- Coropceanu, V.; Malagoli, M.; André, J. M.; Brédas, J. L. *J. Chem. Phys.* **2001**, *115*, 10409.
- For examples of other work recognizing the importance of symmetric modes in the IVCT line shapes of delocalized and nearly delocalized MV systems, see: Reimers, J. R.; Hush, N. S. *Chem. Phys.* **1996**, *208*, 177. Piepho, S. B. *J. Am. Chem. Soc.* **1988**, *110*, 6319. Borrás-Almenara, J. J.; Coronado, E.; Ostrovsky, S. M.; Palii, A. V.; Tsukerblat, B. S. *Chem. Phys.* **1999**, *240*, 149. Bailey, S. E.; Zink, J. I.; Nelsen, S. F. *J. Am. Chem. Soc.* **2003**, *125*, 5939.
- We have previously observed that the IVCT of a delocalized bis(diarylamino)dithienopyrrole radical cation shows a band shape rather different from those of analogues with bithiophene or dithienothiophene bridges (ref 24).
- Optimization of the structures of mixed-valence species typically gives highly methodology-dependent results; electron self-interaction errors in DFT methods tend to afford delocalized structures for open-shell systems, while the neglect of electron correlation effects in

Hartree–Fock (HF) methods often leads to localized solutions: Bally, T.; Borden, W. T. In *Reviews in Computational Chemistry*; Lipkowitz, K., Boyd, D. B., Eds.; Wiley-VCH: New York, 1999; Vol. 13, p 1. Pacchioni, G.; Frigoli, F.; Ricci, D. *Phys. Rev. B* **2000**, *63*, 054102. Kobko, N.; Masunov, A.; Tretiak, S. *Chem. Phys. Lett.* **2004**, *392*, 444. Lundberg, M.; Siegbahn, P. E. M. *J. Chem. Phys.* **2005**, *122*, 224103. Indeed, UB3LYP/6-31G(d) structures (see the Supporting Information) of  $1^+–10^+$  are all symmetric, i.e., suggesting all the species belong to class-III, whereas UHF-AM1 results suggest all belong to class-II. Calculations employing AM1 coupled with CI, to include some degree of electron correlation, can, in some cases, more usefully distinguish between delocalized and localized systems; for example, consistent with experiment, class-II and class-III structures are predicted by AM1/CI calculations for  $4^+$  and its shorter homologue, the (*E*)-4,4'-bis[bis(4-methoxyphenyl)amino]stilbene cation, respectively (ref 25). Recently, hybrid DFT/HF approaches have been used to successfully model (de)localization phenomena in organic MV systems: Renz, M.; Theilacker, K.; Lambert, C.; Kaupp, M. *J. Am. Chem. Soc.* **2009**, *131*, 16292. Kaupp, M.; Renz, M.; Parthey, M.; Stolte, M.; Würthner, F.; Lambert, C. *Phys. Chem. Chem. Phys.* **2011**, *13*, 16973.

(46) On the other hand, we cannot rule out the possibility that  $6^+–8^+$  and  $10^+$  lie in Meyer's "solvent-delocalized" intermediate class-II/III, which can be difficult to experimentally distinguish from class-III: Demadis, K. D.; Hartshorn, C. M.; Meyer, T. J. *Chem. Rev.* **2001**, *101*, 2655.

(47) Indeed, the adiabatic electron-transfer distance,  $R_{12}$ , indicated for the AM1/CI structures for  $1^+$  is considerably greater than the diabatic distance,  $R_{ab}$ , deduced in ref 26 from comparison of optical and VT-ESR data, again suggesting that the AM1/CI structures are overlocalized.

(48) Meyer, T. J. *Acc. Chem. Res.* **1978**, *11*, 94.

(49) The decrease in  $\lambda_0$  predicted between  $1^+$  and  $4^+$  from eq 2 using the AM1/CI values of  $R_{12}$  and assuming the invariant donor and acceptor radii in both cases ( $2970\text{ cm}^{-1}$ ) is somewhat larger than the experimental shift ( $1320\text{ cm}^{-1}$ ). However, the AM1/CI values of  $R_{12}$  are likely overestimates (see ref 47), while the varied deviations of both  $R_{ab}$  and  $R_{12}$  from the geometric N–N distance mean that approximating the redox centers in both cases as triarylaminines is inappropriate.

(50) In the case of significant coupling of the electron-transfer reaction coordinate to symmetric vibrational modes, the coupling is overestimated using eq 3 by a quantity equal to half the relaxation energy associated with the symmetric modes: Coropceanu, V.; Boldyrev, S. I.; Risko, C.; Brédas, J. L. *Chem. Phys.* **2006**, *326*, 107. Although the asymmetry of the IVCT bands of  $6^+–8^+$  is, as previously discussed for other bis(triarylamine) MV systems (refs 19, 41, and 42) attributable to the effects of coupling to symmetric modes, the strength of this coupling decreases rapidly as the size of the system is increased (refs 20, 41, and 51), and the overall IVCT line widths seen for  $6^+–8^+$  are also consistent with much less significant contributions than previously found in shorter species with benzene, biphenyl, and tolane bridges. Thus, the effect of coupling to symmetric modes on  $V$  in the current systems has been neglected.

(51) Risko, C.; Coropceanu, V.; Barlow, S.; Geskin, V.; Schmidt, K.; Gruhn, N. E.; Marder, S. R.; Brédas, J.-L. *J. Phys. Chem. C* **2008**, *112*, 7959.

(52) The calculations fail to correctly reproduce the relative positions of the IVCT maxima of  $6^+$  and  $7^+$  and of  $8^+$  and  $9^+$ ; however, in both of these comparisons there are opposing effects expected, those of bridging and end groups in the first case and of changing the bridging heteroatom and removing alkoxy substituents from the bridge in the latter.

(53) In the case of **9** the HOMO – 2 can be well-described as the corresponding bonding combination, whereas none of the orbitals of **1** can be approximated in such a straightforward fashion (although the HOMO – 2 of **1** still has a considerable contribution from the local bridge HOMO).

(54) Although eq 4 was originally derived at the perturbation limit of weak electronic coupling (ref 3), it was subsequently shown to be

exact within the two-state model regardless of the magnitude of  $V$  (Creutz, C.; Newton, M.; Sutin, N. J. *Photochem. Photobiol.*, **A** **1994**, *82*, 47), at least for cases where only antisymmetric vibrational modes are coupled to the electron transfer. As first pointed out by Hush (Hush, N. S. *ACS Symp. Ser.* **1982**, *198*, 301), however, eq 4 will overestimate the coupling in cases where the electron transfer is also coupled to symmetric modes. As discussed in ref 50, neglect of coupling to symmetric modes is likely to have small effects in the current systems. In particular, these effects are likely to be insignificant compared to the effects of overestimating  $R_{ab}$ , discussed in the text.

(55) Piepho, S. B.; Krausz, E. R.; Schatz, P. N. *J. Am. Chem. Soc.* **1978**, *100*, 2996.

(56) Reimers, J. R.; Hush, N. S. *J. Phys. Chem.* **1991**, *95*, 9773.

(57) Cave, R. J.; Newton, M. D. *Chem. Phys. Lett.* **1996**, *249*, 15.

(58) Veregin, R. P.; Harbour, J. R. *J. Phys. Chem.* **1990**, *94*, 6231.

(59) Duling, D. R. *J. Magn. Reson., Ser. B* **1994**, *104*, 105.

(60) <http://www.niehs.nih.gov/research/resources/software/tox-pharm/tools/index.cfm> (accessed June 4, 2012).

(61) The widths of the simulated spectra depend on the value of the Gaussian line broadening chosen for convolution with the DFT hyperfine constants. However, for small broadenings, sufficient to obscure hyperfine coupling, but much smaller than the overall line width, the line broadening does not affect the pattern of variation between compounds.

(62) Walter, R. I. *J. Am. Chem. Soc.* **1966**, *88*, 1923.

(63) Schmidt, W.; Steckhan, E. *Chem. Ber.* **1980**, *113*, 577.

(64) Robinson, J.; Osteryoung, R. A. *J. Am. Chem. Soc.* **1980**, *102*, 4415.

(65) In the case of  $3^+$  and  $4^+$ , an additional band between the IVCT and "Ar<sub>2</sub>N<sup>+</sup>" absorptions may correspond to a charge transfer from the highest  $\pi$ -bridge-based orbital to the radical cation center (see refs 22, 23, and 25).

(66) For these more delocalized monocations, the bands in this region are somewhat red-shifted from those seen for the class-II species, as previously seen for other class-III bis(diarylamine) MV compounds (refs 10, 18, and 25), and perhaps having a rather different origin (ref 10).

(67) Trace radical signals can arise from some small paramagnetism in the dication, from trace monocation arising from imperfect stoichiometry in the oxidation or from decomposition of the dication, or from trace oxidizing agent arising from imperfect stoichiometry.

(68) For examples of previous studies comparing magnetic coupling in doubly oxidized (or reduced) organic biradicals and the corresponding singly oxidized (or reduced) MV systems, see ref 25. Also see: Nelsen, S. F.; Ismagilov, R. F.; Teki, Y. *J. Am. Chem. Soc.* **1998**, *120*, 2200. Shultz, D. A.; Fico, R. M.; Bodnar, S. H.; Kumar, K.; Vostrikova, K. E.; Kampf, J. W.; Boyle, P. D. *J. Am. Chem. Soc.* **2003**, *125*, 11761. Correlations between magnetic and electronic coupling in homovalent and MV species, respectively, have also been seen in systems with metal-based redox centers; for example: Fabre, M.; Bonvoisin, J. *J. Am. Chem. Soc.* **2007**, *129*, 1434.